April 9-12
Taipei-Taiwan
2019

3rd International Workshop on
Sediment Bypass Tunnels

Analysis of Sediment in the Upper Catchment Area of Shimen Reservoir-Taking Jangmi and Soulik Typhoon as Examples

Yu-Jia Chiu, Hong-Yuan Lee, Tse-Lin Wang

Abstract

1 Introduction

In recent years, typhoons and heavy rains have brought a large amount of sediment into the reservoir from the catchment area, resulting in serious siltation of the reservoir and greatly reducing the reservoir capacity. In order to ensure the function of existing reservoirs and prolong the life of reservoirs, how to estimate the amount of sediment discharge in the upstream catchment area of the reservoir and effective control of the sediment movement mechanism in the upstream catchment area has been the focus of research on the prevention of siltation in the current reservoirs and the sustainable development of reservoir storage capacity.

The research object is the upstream catchment area of Shimen Reservoir. Firstly, the soil water index is simulated by the Tank model to simulate surface runoff and subsurface water content. Combining logistic regression to analyze the landslide potential, the amount of landslide sediment and soil erosion. According to the surface runoff and the amount of sediment production in the slope which simulated by the Tank model the movement phenomenon of surface sand and debris flow is simulated to be used as the inflow of river sediment. In order to provide the boundary, side inflow conditions of the one-dimensional water transport mode, simulate Typhoon event, sand flow, erosion and siltation. Finally, comparing all the simulation results of sediment discharge and the measured data of the reservoir inflow to analyze the sediment inflow discharge in the Shimen Reservoir.

Keywords: sediment yield; sediment transport mechanism; Shihmen Reservoir catchment

2 Materials and Methods

Shimen Reservoir (Fig. 1) is located in the upper reaches of Dahan stream, Taiwan, with a total area of 766 km^2, altitude from 135 m to 3,500 m. The slope of the catchment area is dominated by 6 grades, the annual average rainfall is 2,370 mm and the rainfall is concentrated on May every year. The area of research is from Hsiayun water level station to Luofu Bridge. Through the collection of basic data, we estimated the amount of landslide sediment and use hydrological model to estimate the inflow of river as the boundary condition of flow and sediment transport model. The flow and sediment model

is used to simulate the sediment movement of the typhoon event, and comparing the simulation results of the downstream (Luofu) sediment discharge and the measured data of the reservoir inflow (Luofu) sediment discharge. The research process is shown in Fig. 2.

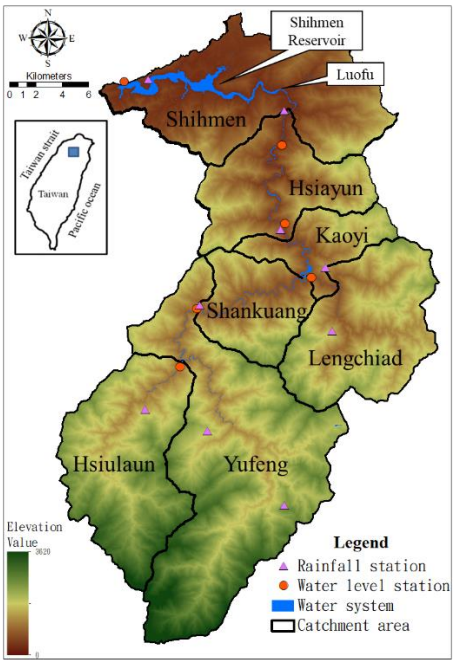

Fig. 1: Research Area

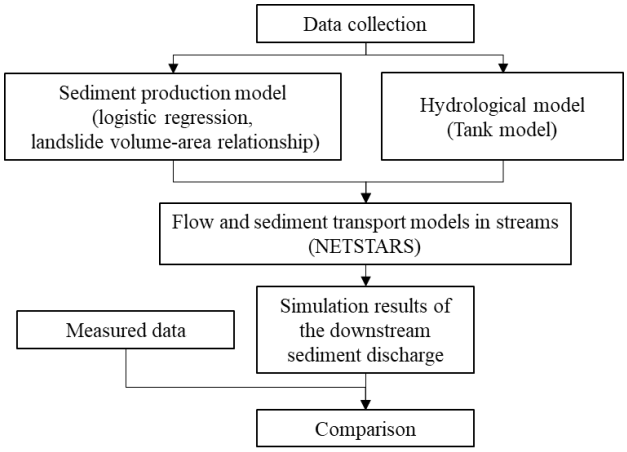

Fig. 2: Work Flow Chart

The numerical model were used in the catchment area includes the hydrological model of upstream water flow discharge supply, the sediment production model of sediment discharge supply and the flow and sedimen model of bed change. The model descriptions are as following.

2.1 Hydrological model

The water tank model is a conceptual model simulating the movement behavior of runoff, infiltration and seepage. Okada (2002) which divided the model into three layers, can be regarded as the surface layer. The middle layer and the deep soil layer. The sum of the water depths of the three layers is called the soil water index (SWI). Based on the tank model, this study uses the Hsiayun water level station to verify the accuracy and correct it by the coefficient of efficiency (CE) standard. The calculation formula is as follows:

$$CE = 1 - \frac{\sum_{i-1}^{n} \left[Q_{obs}(i) - Q_{est}(i) \right]^2}{\sum_{i-1}^{n} \left[Q_{obs}(i) - \overline{Q}_{obs}(i) \right]^2} \quad [1]$$

Where Qest is the flow discharge estimated by the model; Qobs is the observed flow discharge, which is the average of the observed flow discharge. The CE value is closer to 1, it is shown that the simulation results were closer to the actual data and more precisely.

Figure 3(a) shows the calibration results of the Fanapi typhoon flow discharge in 2009, which using the water tank model. There are good results in the simulated flood peak flow and the flow change in the dewatering section, and the efficiency coefficient is 0.93. Figure 3(b) shows the verification results of the Fanapi typhoon flow discharge in 2010. The simulated and observed peak flow is quite close. There are still good simulation results in the second half of the retreat, but there is a slightly overestimated phenomenon. The overall simulation results are quite good with an efficiency factor of 0.90, so it can be applied to estimate runoff and soil water index estimates.

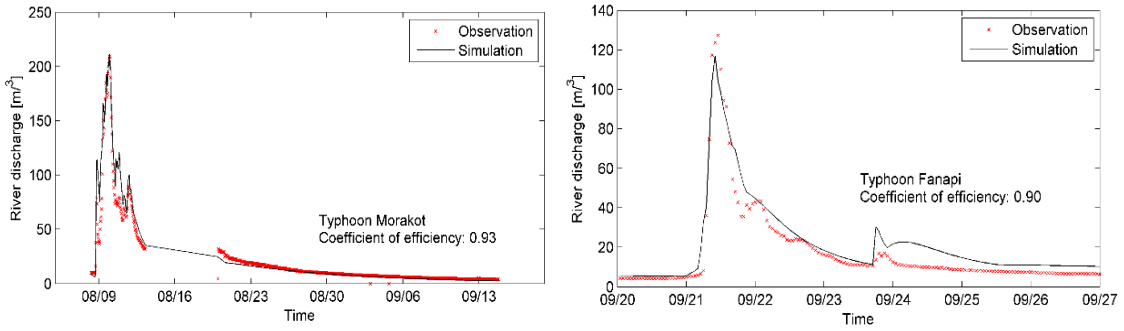

(a) Morakot Typhoon Flow Rate Results (b) Fanapi Typhoon Flow Rate Results

Figure .3: Results of hydrological analysis mode calibration, verification

2.2 Sediment production model

2.2.1 Landslide potential

The study uses logistic regression to assess the landslide potential and the soil water index as a hydrological factor. Simulate the physical phenomena caused by pores or groundwater pressure, and simulate the dynamic process of landslide. Put each parameter that affects the landslide factor into the logistic regression, and calculate the coefficients of each parameter to get the formula 2:

$$P = \frac{\exp(Logit(y))}{1+\exp(Logit(y))} = \frac{\exp(a+b_1x_1+b_2x_2+b_3x_3+...)}{1+\exp(a+b_1x_1+b_2x_2+b_3x_3+...)} \quad [2]$$

Among them, P is the probability of occurrence of collapse, y is an independent variable, x_i is an explanatory variable, and b_i is a regression coefficient.

Based on the multi-temporal (event-based landslide inventory), the 2004 Aere typhoon rate model parameters, and then the 2005 Matsa typhoon to verify the success rate of the collapse prediction. Finally, the accuracy of the landslide area was calibrated and verified

with the landslide area of ten typhoons. The AUC (area under curve) is 0.79; the simulated AUC of the Martha Typhoon is 0.74, indicating that the model has acceptable explanatory power (Fig. 4(a)). Figure 4(b) shows that this model simulates the new landslide areas of the ten typhoon events and has a good performance. Based on the landslide probability model, the spatial distribution of the maximum soil water index of Typhoon Aere in 2004 and Typhoon Matsa in 2005 can be used to calculate the prediction results of the collapse probability of the two typhoon events, as shown in Figure 5.

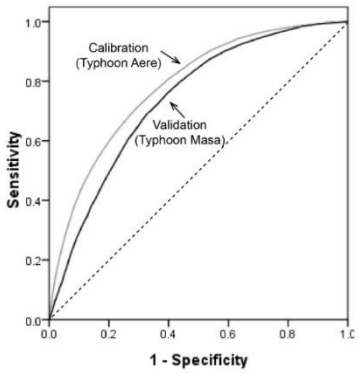

(a) ROC Curve verification Avery and Martha Typhoon

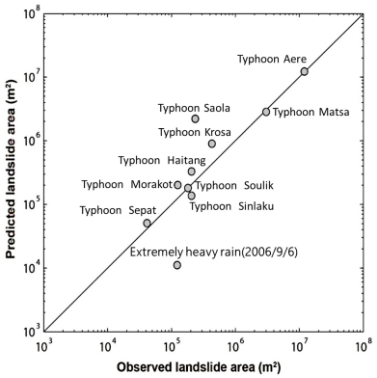

(b)The new collapse area verification

Fig.4: Typhoon event success rate curve and new collapse area verification results

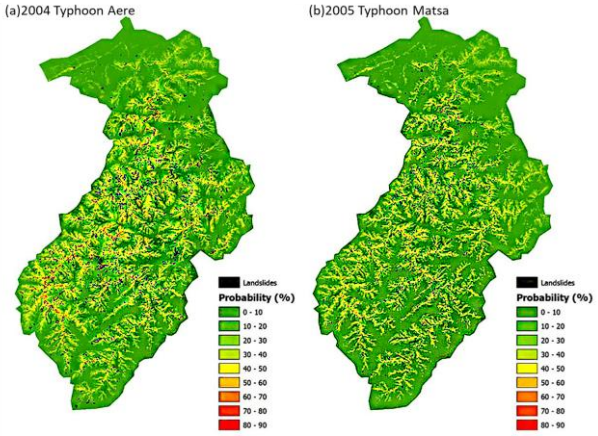

Fig.5: Typhoon collapse rate prediction results

2.2.2 Sediment production

From the analysis results of landslide potential, the location, size and quantity of landslide in the catchment area can be obtained. In order to further evaluate the amount of slope landslide, this study used the landslide volume-area relationship formula to estimate the amount of hillside landslide sediment. The relationship is:

$$V_L = 0.458 \times A_L^{1.179} \quad [3]$$

Among them, V_L is the collapse volume [m^3]; A_L is the collapse area [m^2], and the relational coefficient (R^2) is 0.94, which means that the relationship has good interpretation ability. The calculation of soil erosion is based on the Modified Soil Loss Equation. The advantage is that it can simulate a single rainstorm event. The calculation formula is as shown in Equation 4:

$$V_s = 11.8(V_{eff} \times Q_p)^{0.56} \times K_m \times LS \times C \times P \quad [4]$$

V_s is the amount of soil loss [tons]; V_{eff} is the effective runoff [m^3]; Q_p is the peak runoff [cms]; K_m is the soil erosion index (tons × hectares × hours / 106 joules - mm - hectares); L_S is the topographic factor; C is the coverage and management factor; P is the soil and water conservation factor.

2.2.3 Sediment transport

Sediment transport on the slope has two phenomena: debris flow and runoff erosion. The movement behavior of earth-rock flow is controlled by gravity factor, the behavior of runoff scour is controlled by runoff, and the two are different sports behaviors. During the typhoon, two kinds of sediment transport behaviors usually occur at the same time. Therefore, when simulating the sediment transport, the effects of the two should be considered at the same time. The following analysis of the analysis method of this study:

The slope runoff simulation is based on the simple runoff model of Ye (2003). Using the numerical elevation model grid as the unit of calculation, a two-dimensional distributed rainfall runoff model is established to provide the slope runoff of the slope soil and sand migration to the river.

The surface scouring is based on Xie (1998) amendment to Takahashi's (1981) equilibrium sediment concentration formula. The sediment transport concentration under various slopes is proposed, which is suitable for the estimation of sediment transport in the upstream catchment area of mountainous areas.

The debris flow simulation is based on the fully laminar flow which developed by Jiang (2010) and Hunt (1994).

2.3 Flow and sediment transport models in streams

This study uses the NETSTARS model to simulate the amount of sediment transported in the Dahan stream upstream of the Shimen Reservoir.And using the 2015 cross section data to simulate the 2008 Sinlaku typhoon and the 2009 Morakot typhoon. Deterring the sediment discharge in the downstream Luofu (section 3) and the measured inflow sediment discharge in the Shimen Reservoir. The comparison results are shown in Figures 6(a) and (b). The error of peak sediment discharge is about 7%~15%, and the change trend of sediment discharge is similar.

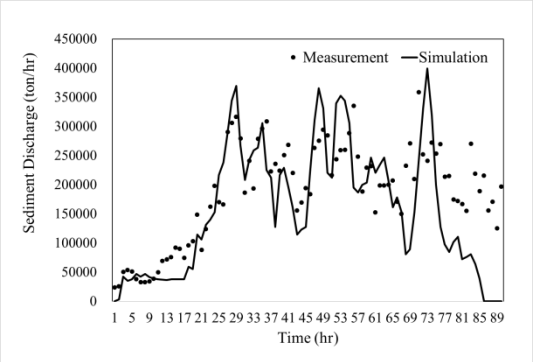

(a) Xinleke typhoon sand yield rate results

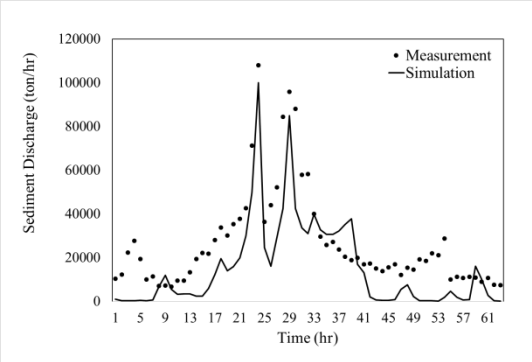

(b) Morakot typhoon sand production verification results

Fig.6: Sand output rate determination, verification results

3 Results

The research is used the cross section measurement data as the initial bed in 2015,using NETSTARS model to simulate Jangmi typhoon in 2008 and Soulik typhoon in 2013. The boundary conditions are shown in Figure 7 and Figure 8. The comparison results of the simulation results (Luofu) and the measured sediment transport data are shown in Figure 9. In general, the change trend of sediment discharge is similar. The error of peak sediment discharge is about 12%~20%, and the sediment discharge in the retreating section was underestimated slightly.

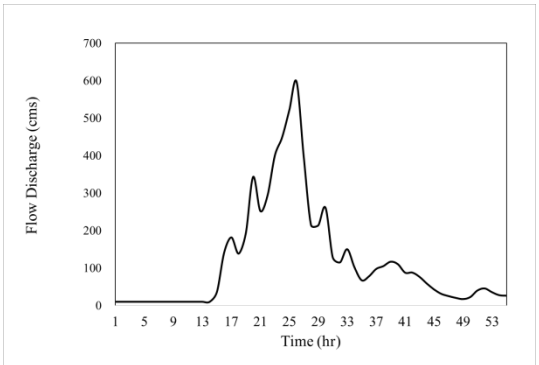

(a)Flow

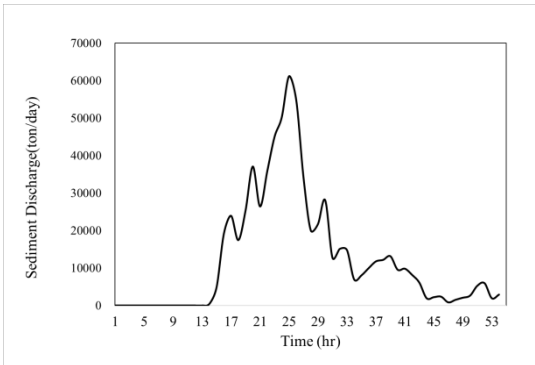

(a) Sand input

Fig.7: The boundary condition of Jangmi

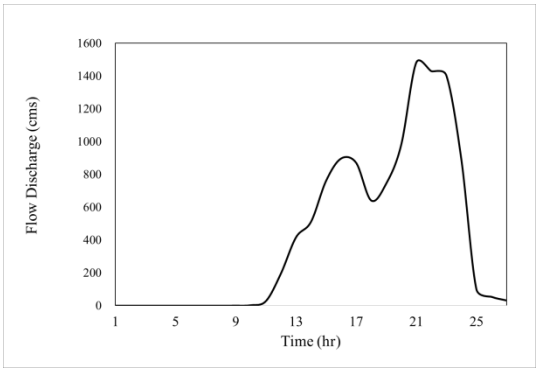

(a) Flow

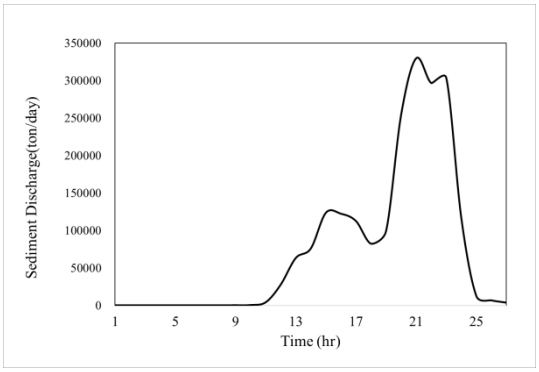

(a) Sand input

Fig.8: The boundary condition of Soulik

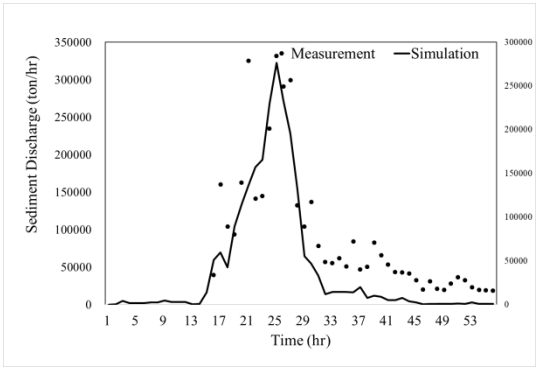

(a) Jangmi typhoon

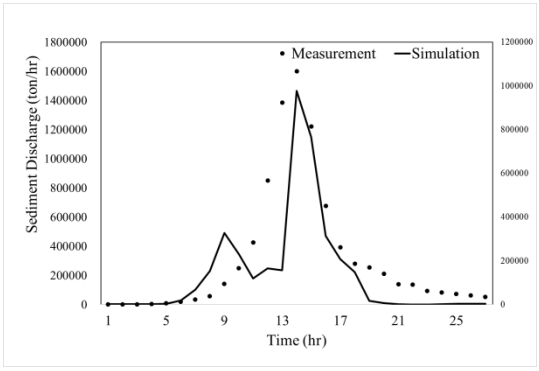

(b) Soulik typhoon

Fig.9: Simulation results of Luofu sand transporting volume and comparison results of measured sediment yield in storage

4 Conclusions

(1) The soil water index is simulated by the Tank model to simulate surface runoff and subsurface water content. Combining logistic regression to analyze the landslide potential, the amount of landslide sediment and soil erosion.

(2) The landside probability model simulates the AUC of Aere typhoon is 0.79 and the the AUC of the Matsa typhoon is 0.74, indicating that the model has acceptable interpretation capabilities.

(3) The sediment production model simulates the migration of sediment by surface erosion and earth-rock flow. Providing the boundary conditions of flow and sediment transport models in streams to simulate the behavior of silt-sinking water.

(4) According to the Luofu (section 3) calibration and verification results of sediment discharge. The error of peak sediment discharge is about 7%~15%, and the change trend of sediment discharge is similar.

(5) Using NETSTARS model to simulate the Jangmi typhoon and the Soulik typhoon. The error of peak sediment discharge is about 12%~20%, and the sediment discharge in the retreating section is slightly underestimated.

Acknowledgement

This research was funded by National Science Council of Taiwan [grant number NSC 105-2221-E-002-063-MY3].

References

1. Ayalew, L., Yamagishi, H. (2004). Ugawa, N. Landslide susceptibility mapping using GIS-based weighed linear combination, the case in Tsugawa area of Agano River, Niigata Prefecture, Japan. *Landslides,* 1, 73-81.
2. Ayalew, L., Yamagishi, H. (2005). The application of GIS-based logistic regression for landslide susceptibility mapping in the Kakuda-Yahiko Mountains, Central Japan. *Geomorphology,* 65, 15-31.
3. Beven, K.J., Kirkby, M.J. (1979). A physically based, variable contributing area model of basin hydrology. *Hydrol. Sci. B,* 24, 43-69.
4. Cooper, V.A., Nguyen, V.T.V. *et al.* (1997). J.A Evaluation of global optimization methods for conceptual rainfall–runoff model calibration. *Water Sci. Technol*, 36(5), 53-60.
5. Chang, K. (2005). Introduction to Geographic Information Systems, Sage: McGraw-Hill, New York, U.S.A, 3rd ed.
6. Chang, K.T., Chiang, S.H. *et al.* (2007). Modeling typhoon- and earthquake-induced landslides in a mountainous watershed using logistic regression. *Geomorphology,* 89(3), 335-347.
7. Chang, K.Y., Chiang, S.H. (2009). An integrated model for predicting rainfall-induced landslides. *Geomorphology,* 105, 366-373.
8. Chen, S.K., Chen, R.S., *et al.* (2014). Application of a tank model to assess the flood-control function of a terraced paddy field. *Hydrolog. Sci. J*, 59(5), 1020-1031.
9. Ikeya, H. (1981). Symposium on Erosion and Sediment Transport in Pacific Rim Steeplands; IAHS Publ. Christchurch, N.Z. , vol. 132.
10. Liu, C.-Y., Lin, W.-T. *et al.* (2002). Soil erosion prediction and sediment yield estimation: the Taiwan experience. *Soil Till. Res,* 68(2), 143-152.
11. Lee, H.-Y., Hsieh, H.-M. (2003). Numerical simulations of scour and deposition in a channel network. *Int. J. Sediment Res,* 18(1), 32-49.
12. Larsen, I.J., Montgomery, D.R. *et al.* (2010). Landslide erosion controlled by hillslope material. Nat. Geosci, 3(4), 247-251.
13. Liu, Y.-H., Li, D.-H. *et al.* (2018). Soil erosion modeling and comparison using slope units and grid cells in Shihmen Reservoir watershed in northern Taiwan. *Water,* 10, 1387.
14. Menard, S. (2002). Applied Logistic Regression Analysis, Sage: Thousand Oaks, CA, U.S.A, 2nd ed.

15. National Land Surveying and Mapping Center. (2012).Report of the Second National Land Use Survey; National Land Surveying and Mapping Center: Taichung, Taiwan.

16. Okada, K. (2002). Soil Water Index. *Weather Serv. Bull*, 69(5), 67-97.

17. Oku, Y., Yoshino, J. *et al.* (2014). Assessment of heavy rainfall-induced disaster potential based on an ensemble simulation of Typhoon Talas (2011) with controlled track and intensity. *Nat. Hazard Earth Sys*, 14(10), 2699-2709.

18. Pontius Jr., R.G., Batchu, K. (2003). Using the relative operating characteristic to quantify certainty in prediction of location of land cover change in India. *T GIS*, 7, 467-484.

19. Quinn, P.F., Beven, K.J. *et al.* (1995). Lamb, R. The ln(a/tanβ) index: how to calculate it and how to use it within the TOPMODEL framework. *Hydrol. Process*, 9, 161-182.

20. Sugawara, M. (1995). In Computer Models of Watershed Hydrology, Singh. V.P. Ed. Water Resources Publications, Colorado, U.S.A.1st ed.

21. Suryoputro, N., Suhardjono. *et al.* (2017). Calibration of infiltration parameters on hydrological tank model using runoff coefficient of rational method. *Proceedings of the Green Construction and Engineering Education.*: 020056.

22. WRPI (Water Resource Planning Institute). (2010). A Study of Flood control and Sediment Management due to Climate Change of Tamsui River (1/2); Taiwan Water Resource Agency Report, Taipei.

Authors

Yu-Jia Chiu[2,*]
Hong-Yuan Lee[1,2]
Tse-Lin Wang[2]
[1]Dept. of Civil Engineering, National Taiwan University, Taipei, 106, Taiwan
[2]Hydrotech Research Institute, National Taiwan University (NTU), Taiwan
*Email:yujiachiu@ntu.edu.tw